LETTER

doi:10.1038/nature11368

Genotoxic consequences of endogenous aldehydes on mouse haematopoietic stem cell function

Juan I. Garaycoechea[1]*, Gerry P. Crossan[1]*, Frederic Langevin[1], Maria Daly[1], Mark J. Arends[2] & Ketan J. Patel[1,3]

Haematopoietic stem cells (HSCs) regenerate blood cells throughout the lifespan of an organism. With age, the functional quality of HSCs declines, partly owing to the accumulation of damaged DNA[1–3]. However, the factors that damage DNA and the protective mechanisms that operate in these cells are poorly understood. We have recently shown that the Fanconi anaemia DNA-repair pathway counteracts the genotoxic effects of reactive aldehydes[4,5]. Mice with combined inactivation of aldehyde catabolism (through *Aldh2* knockout) and the Fanconi anaemia DNA-repair pathway (*Fancd2* knockout) display developmental defects, a predisposition to leukaemia, and are susceptible to the toxic effects of ethanol—an exogenous source of acetaldehyde[4]. Here we report that aged *Aldh2*$^{-/-}$ *Fancd2*$^{-/-}$ mutant mice that do not develop leukaemia spontaneously develop aplastic anaemia, with the concomitant accumulation of damaged DNA within the haematopoietic stem and progenitor cell (HSPC) pool. Unexpectedly, we find that only HSPCs, and not more mature blood precursors, require *Aldh2* for protection against acetaldehyde toxicity. Additionally, the aldehyde-oxidizing activity of HSPCs, as measured by Aldefluor stain, is due to Aldh2 and correlates with this protection. Finally, there is more than a 600-fold reduction in the HSC pool of mice deficient in both Fanconi anaemia pathway-mediated DNA repair and acetaldehyde detoxification. Therefore, the emergence of bone marrow failure in Fanconi anaemia is probably due to aldehyde-mediated genotoxicity restricted to the HSPC pool. These findings identify a new link between endogenous reactive metabolites and DNA damage in HSCs, and define the protective mechanisms that counteract this threat.

Reactive aldehydes, such as acetaldehyde, are by-products of metabolism. These molecules readily react with DNA and proteins within cells, leading to both mutagenesis and cell death[4]. Recent work has identified a critical requirement for the aldehyde-catabolising enzyme Aldh2 and the Fanconi anaemia DNA-repair pathway in protecting against damage caused by these toxic molecules. The majority of mice deficient in both acetaldehyde catabolism (*Aldh2*$^{-/-}$) and the Fanconi anaemia DNA-repair pathway (*Fancd2*$^{-/-}$), spontaneously succumb to acute T-cell leukaemia[4]. Flow cytometric analysis revealed that the maturation of haematopoietic lineages was intact (Supplementary Fig. 1). However, double-mutant mice, without leukaemia, consistently have reduced numbers of all blood constituents and bone marrow cellularity, compared to wild-type controls (Supplementary Fig. 2). Furthermore, a small proportion of these double-mutant mice developed anaemia with age ($n = 6/29$) (Fig. 1a). These mice showed profound pancytopenia, and histological analysis of the bone marrow revealed hypocellularity (Fig. 1b, c and Supplementary Fig. 3a). Furthermore, these mice showed extramedullary haematopoiesis (Supplementary Fig. 3b). These clinical and pathological features are consistent with aplastic anaemia—a hallmark of human Fanconi anaemia but, until now, not a feature observed in Fanconi anaemia knockout mice. Immunohistochemistry revealed that the bone marrow of the aged *Aldh2*$^{-/-}$ *Fancd2*$^{-/-}$ mice had increased numbers of cells that were positive for γ-H2AX, a well-established marker of DNA double-strand breaks[6]. There was also an increased proportion of cells undergoing apoptosis, as measured by cleaved caspase-3 (Fig. 1c). The data in Fig. 1d, e show that there was a significant induction in γ-H2AX, as measured by flow cytometry, within the total bone marrow of aged aplastic double-mutant mice. However, γ-H2AX induction within the Lineage (Lin)$^-$ c-Kit$^+$ Sca-1$^+$ (LKS) population, which is enriched for HSPCs, was much greater. Analysis of young *Aldh2*$^{-/-}$ *Fancd2*$^{-/-}$ mice indicated that the induction in γ-H2AX was greater in long-term HSCs (LT-HSCs; Lin$^-$ c-Kit$^+$ Sca-1$^+$ Flt3$^-$ CD34$^-$) than in other haematopoietic progenitors (Supplementary Fig. 4). Taken together this suggests that there is a requirement for acetaldehyde catabolism and Fanconi anaemia pathway-mediated DNA repair for blood homeostasis, and that this activity may be restricted to a subset of haematopoietic cells.

We therefore set out to test systematically how haematopoietic cells at different stages of maturity respond to exogenous acetaldehyde—the key substrate of Aldh2. In the first instance we found that B cells, erythroid progenitor and granulocyte–macrophage progenitor cells from three different strains of mice deficient in the Fanconi anaemia DNA-repair pathway (*Fanca*$^{-/-}$, see Supplementary Fig. 5; *Fancd2*$^{-/-}$, ref. 7; and *Fancp*$^{-/-}$ (*Fancp* is also known as *Slx4*); ref. 8) were all more sensitive to acetaldehyde than congenic controls (Fig. 2a). Surprisingly, when we tested the resistance of haematopoietic cells deficient in both *Aldh2* and *Fancd2*, we noted that all three lineages tested were no more sensitive than those deficient in *Fancd2* alone (Fig. 2b). In contrast, we have previously shown that *Aldh2*$^{-/-}$ *Fancd2*$^{-/-}$ mice developed bone marrow failure after ethanol exposure, but that this did not occur in single-mutant mice[4]. We speculated that this was because aldehyde catabolism and the Fanconi anaemia repair pathway specifically protected the HSC compartment, and therefore aldehyde accumulation would be most toxic to this vital cell population. Progressive attrition of the HSC pool is considered to be the reason why most Fanconi anaemia patients develop bone marrow failure[9].

To test this, we modified the classic colony-forming unit spleen (c.f.u.-S) assay, which is used to quantify short-term HSCs (ST-HSCs), a subset of HSPCs[10–12]. As shown in Fig. 2c, we exposed the bone marrow of mutant and wild-type mice to acetaldehyde *in vitro*, before transplantation into lethally irradiated recipients. Ten days after transplantation we killed the mice and counted the number of spleen colonies. This assay therefore allows us to measure directly the survival of ST-HSCs after exposure to acetaldehyde. The data in Fig. 2d show that ST-HSCs use both aldehyde detoxification and Fanconi anaemia pathway-mediated DNA repair to counteract the genotoxic effects of acetaldehyde. This is in contrast to the more mature haematopoietic cells, in which *Aldh2* is dispensable for resistance to acetaldehyde.

For many years it has been appreciated that potent aldehyde dehydrogenase activity is associated with certain normal and cancer stem cells[13–15]. This activity can be quantified by the commercial assay

[1]MRC Laboratory of Molecular Biology, Hills Road, Cambridge CB2 0QH, UK. [2]University of Cambridge, Department of Pathology, Addenbrooke's Hospital, Cambridge CB2 2QQ, UK. [3]University of Cambridge, Department of Medicine, Level 5, Addenbrooke's Hospital, Cambridge CB2 0QQ, UK.
*These authors contributed equally to this work.

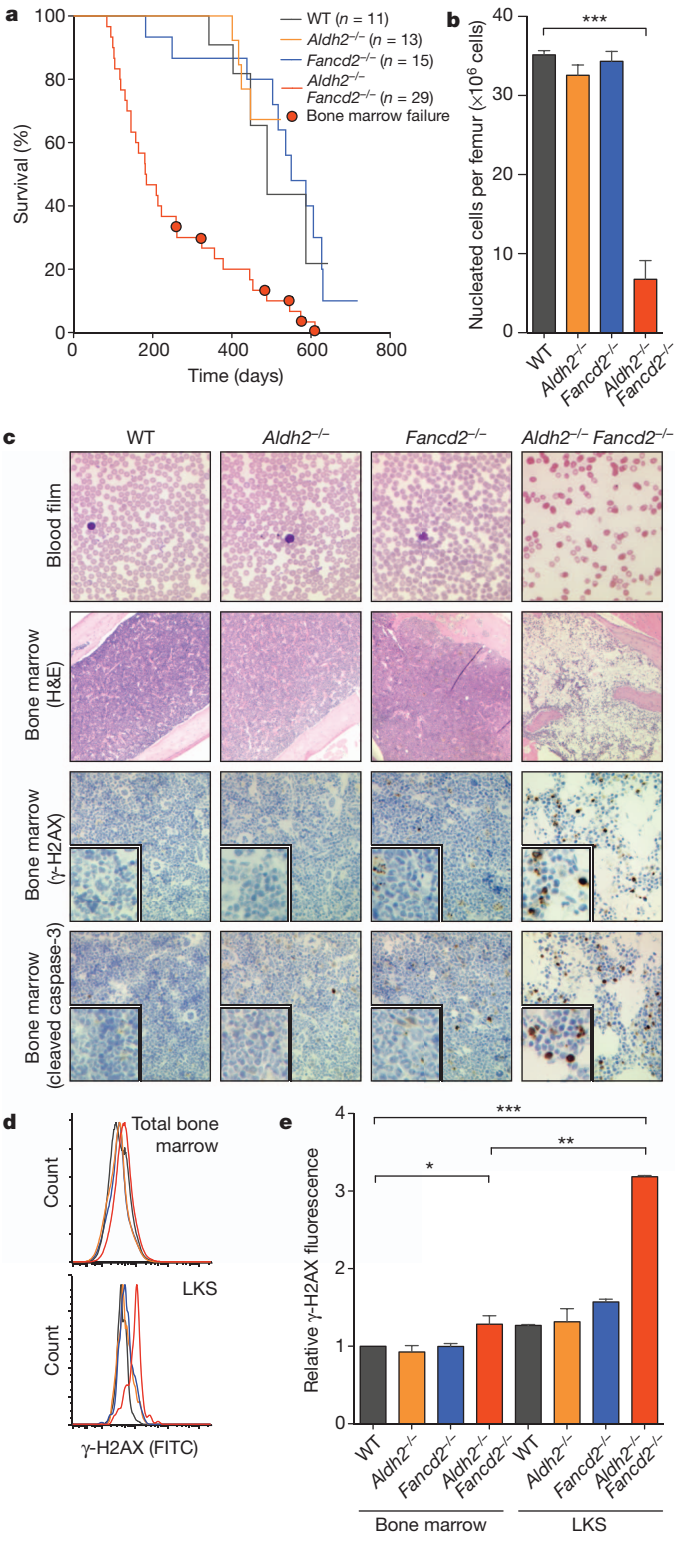

Figure 1 | Aged *Aldh2*$^{-/-}$ *Fancd2*$^{-/-}$ mice succumb to bone marrow failure. **a**, Kaplan–Meier curve showing the survival of a cohort of *Aldh2*$^{-/-}$ *Fancd2*$^{-/-}$ mice and congenic controls. Red dots denote mice with bone marrow failure ($n = 6/29$). WT, wild type. **b**, Bar chart representing the number of nucleated cells per femur of aged *Aldh2*$^{-/-}$ *Fancd2*$^{-/-}$ mice ($n = 6$) with bone marrow failure and controls. Error bars represent s.e.m. **c**, Peripheral blood film (×400), bone marrow histology stained with haematoxylin and eosin (H&E; ×50) and immunohistochemistry for cleaved caspase-3 or γ-H2AX (×200, inset ×400) from an *Aldh2*$^{-/-}$ *Fancd2*$^{-/-}$ mouse with bone marrow failure and controls. **d**, **e**, Flow cytometric analysis of γ-H2AX in total bone marrow and LKS populations with quantification of the relative induction in *Aldh2*$^{-/-}$ *Fancd2*$^{-/-}$ (error bars represent s.e.m., $n = 2$, $^{*}P < 0.05$, $^{**}P < 0.01$, $^{***}P < 0.001$).

known as Aldefluor[16]. Briefly, cells are incubated with a fluorescent aldehyde substrate that, when oxidized by aldehyde dehydrogenases, cannot efflux from the cell (Fig. 3a). The amount of fluorescence reflects the aldehyde dehydrogenase activity in that cell. The addition of 4-diethylaminobenzaldehyde (DEAB), which is an inhibitor of Aldh enzymes, prevents enzymatic oxidation and the accumulation of this product, therefore providing a negative control for fluorescence. In human bone marrow, the Aldefluor activity of HSCs is sufficient to enable their identification and isolation[16]. However, the restriction of this aldehyde dehydrogenase activity to the HSC pool seems to be less strict in mouse than in man[17,18]. The identity of the enzyme responsible for Aldefluor activity was unknown, although it has recently been shown that it is not due to *Aldh1a1* (ref. 17). In contrast, we find that the Aldefluor activity is greatly abrogated in *Aldh2*$^{-/-}$ mice. There is a marked reduction in the Aldefluor activity of total bone marrow and of the HSPC pool, with an intermediate reduction in *Aldh2*$^{+/-}$ mice (Fig. 3b, c). Furthermore, Aldh2 is the most highly expressed member of the aldehyde dehydrogenase family in the LT-HSC population[17,19]. These data suggest that Aldh2 is the major source of Aldefluor activity and acetaldehyde detoxification within the HSPC pool.

Having established that *Aldh2* and *Fancd2* protect HSPCs against acetaldehyde-mediated genotoxicity, we set out to establish the direct physiological consequences of disruption of both genes on HSPC function in young 8–12-week-old mice. First we used immunophenotyping to determine the frequency of HSPCs within the bone marrow of young double-mutant mice that had not developed leukaemia or bone marrow failure[20–22]. The data in Fig. 4a show a 30-fold reduction in the LKS population, in contrast to the mild twofold reduction in *Fancd2*$^{-/-}$ mice. Further analysis of this population revealed that there was a tenfold reduction in the frequency of LT-HSCs (Lin^{-} c-Kit^{+} $Sca\text{-}1^{+}$ $Flt3^{-}$ $CD34^{-}$) in *Aldh2*$^{-/-}$ *Fancd2*$^{-/-}$ mice compared to wild-type littermates, with *Fancd2*$^{-/-}$ or *Aldh2*$^{-/-}$ mice again showing only a mild reduction (Fig. 4b and Supplementary Fig. 6a). Similarly, bone marrow from *Aldh2*$^{-/-}$ *Fancd2*$^{-/-}$ mice showed a significant reduction in the frequency of HSCs defined by SLAM markers (Lin^{-} $CD41^{-}$ $CD48^{-}$ $CD150^{+}$)[19]. However, when SLAM markers were combined with canonical HSC surface markers (SLAM + LKS: Lin^{-} $CD41^{-}$ $CD48^{-}$ $CD150^{+}$ c-Kit^{+} $Sca\text{-}1^{+}$), a more pronounced 251-fold reduction in the frequency of HSCs was observed in *Aldh2*$^{-/-}$ *Fancd2*$^{-/-}$ mice (Supplementary Fig. 6b–d).

Analysis of cell cycle dynamics revealed an accumulation in the S–G2–M phase of the cell cycle in double-mutant LT-HSCs. Furthermore, we noticed a marked reduction in the number of quiescent (G_0) LT-HSCs in *Aldh2*$^{-/-}$ *Fancd2*$^{-/-}$ mice ($P < 0.0001$). The majority of LT-HSCs were actively cycling, in contrast to wild-type LT-HSCs, which are mainly quiescent (Fig. 4c). It has previously been demonstrated that damage to the bone marrow compartment leads to a loss of quiescence and entry of HSCs into the cell cycle[21,23,24].

Finally, we functionally tested the HSPC pool of young *Aldh2*$^{-/-}$ *Fancd2*$^{-/-}$ mice. Bone marrow obtained from *Aldh2*$^{-/-}$ *Fancd2*$^{-/-}$ mice and congenic controls was transplanted into lethally irradiated recipients. These recipients were then killed at day 10 and the number of spleen colony forming units (c.f.u.-S_{10}) was quantified. The data in Fig. 4d and Supplementary Fig. 7a clearly show that the number of c.f.u.-S_{10} was greatly reduced (28-fold) in mice reconstituted with *Aldh2*$^{-/-}$ *Fancd2*$^{-/-}$ marrow compared with wild type, in contrast to the mild reductions in the single mutants (*Aldh2*$^{-/-}$, 1.8-fold; *Fand2*$^{-/-}$, 3.2-fold compared with wild type). The *in vitro* cobblestone-area-forming cell (CAFC) assay corroborates this decreased frequency of HSPCs in *Aldh2*$^{-/-}$ *Fancd2*$^{-/-}$ marrow (Supplementary Fig. 7b). However, these assays have limitations because we cannot draw any conclusions about the long-term repopulating potential of the HSCs. To assess this function, we carried out the

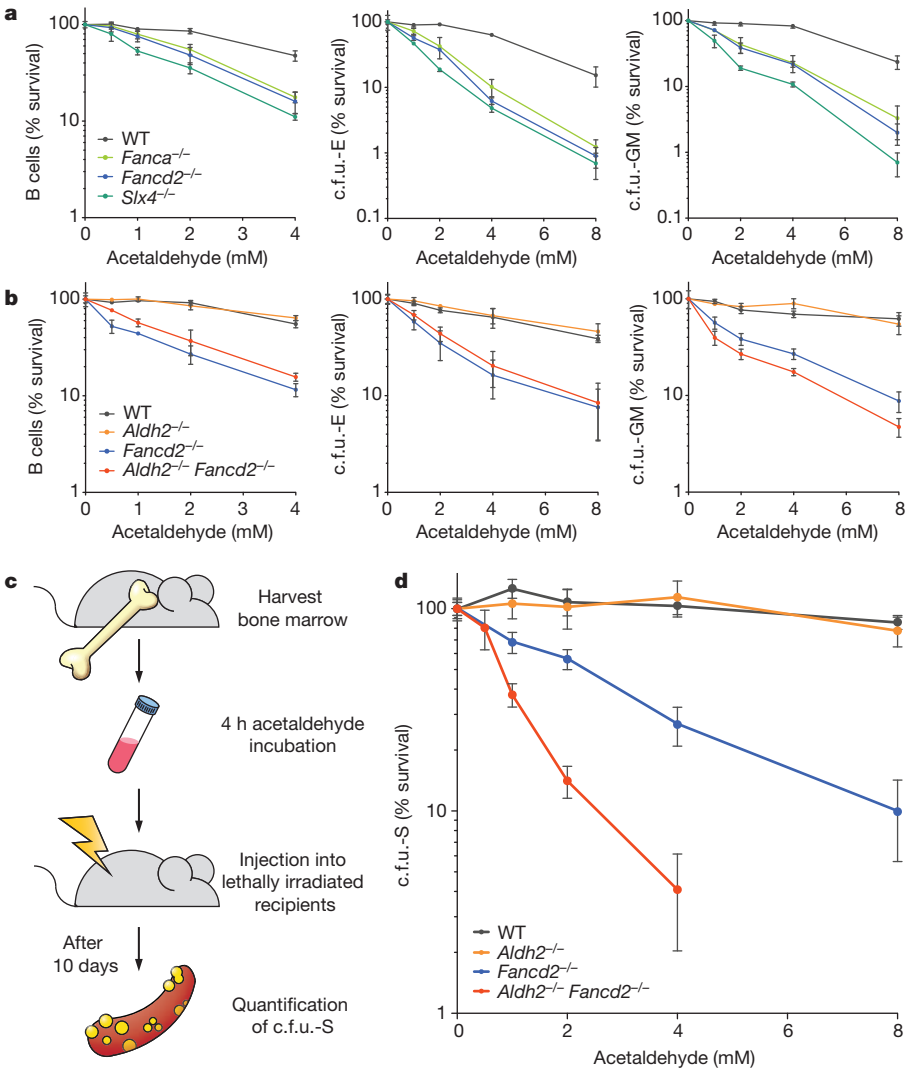

Figure 2 | *Aldh2* is critical for protecting *Fancd2*$^{-/-}$ ST-HSCs from exogenous acetaldehyde. **a**–**d**, Survival of B cells, eyrthroid (c.f.u.-E) and granulocyte–macrophage (c.f.u.-GM) progenitors following exposure to acetaldehyde *in vitro*. **a**, **b**, Cells were obtained from wild-type (WT), *Fanca*$^{-/-}$, *Fancd2*$^{-/-}$ and *Slx4*$^{-/-}$ mice (**a**) or wild-type, *Aldh2*$^{-/-}$, *Fancd2*$^{-/-}$ and *Aldh2*$^{-/-}$ *Fancd2*$^{-/-}$ mice (**b**). Each data point represents the mean of two independent experiments, each carried out in duplicate, error bars represent s.e.m. **c**, Scheme outlining the assay to determine survival of ST-HSCs (c.f.u.-S_{10}) after exposure to acetaldehyde. **d**, c.f.u.-S_{10} survival was made relative to the untreated controls of each genotype. Each data point represents the mean c.f.u.-S_{10} survival among eight recipient mice. Error bars represent s.e.m.

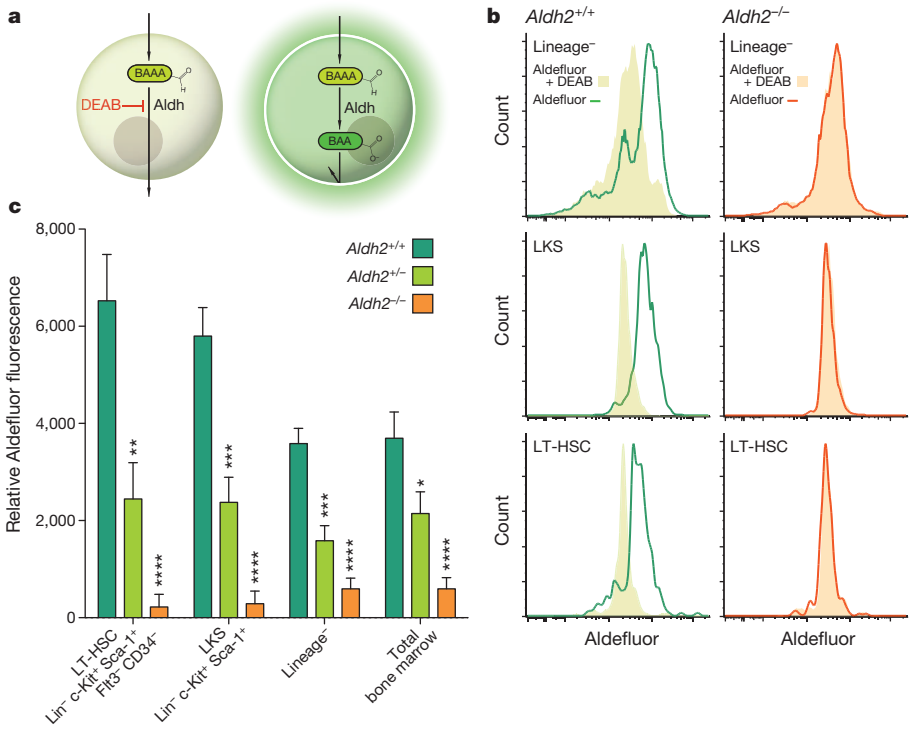

Figure 3 | Aldh2 is responsible for Aldefluor activity in murine HSPCs. **a**, Scheme outlining the Aldefluor assay. The substrate is oxidized by Aldh enzymes and the charged fluorescent product accumulates. DEAB, a general inhibitor of Aldh enzymes, was used as a control for background fluorescence. **b**, Flow cytometric analysis of the lineage-negative, LKS and long-term HSC (LT-HSC) populations of *Aldh2*$^{+/+}$ and *Aldh2*$^{-/-}$ bone marrow treated with the Aldefluor reagent with and without DEAB. **c**, Quantification of Aldefluor fluorescence in bone marrow subpopulations from *Aldh2*$^{+/+}$, *Aldh2*$^{+/-}$ and *Aldh2*$^{-/-}$ mice. The data were made relative to DEAB control and represents the mean of three independent experiments. Error bars represent s.e.m., $n = 10$, $^{*}P < 0.05$, $^{**}P < 0.01$, $^{***}P < 0.001$ and $^{****}P < 0.0001$ compared with *Aldh2*$^{+/+}$ control for each population.

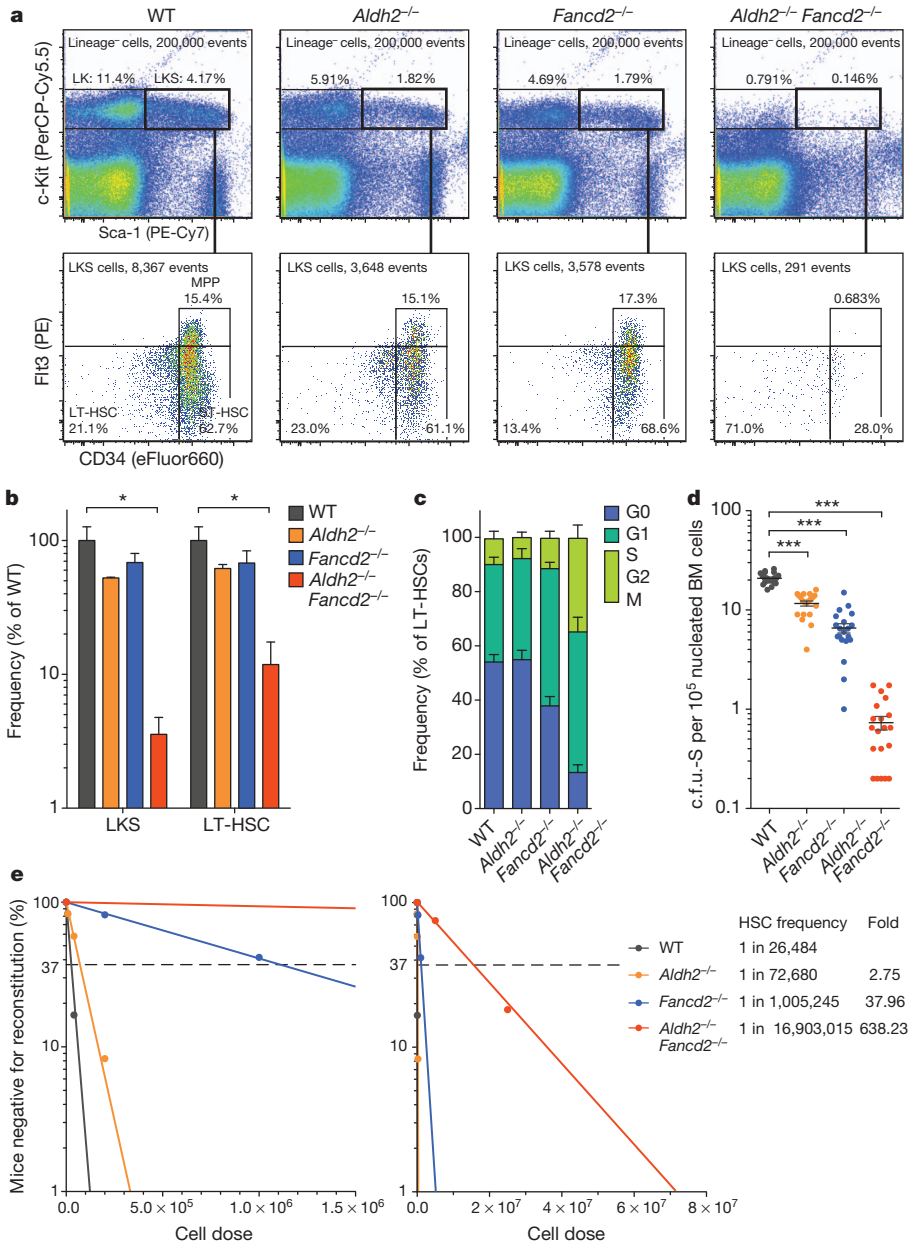

Figure 4 | The HSC pool of young *Aldh2*$^{-/-}$ *Fancd2*$^{-/-}$ mice is severely compromised. a, Representative FACS profiles of HPSCs of 8–12-week-old *Aldh2*$^{-/-}$ *Fancd2*$^{-/-}$ mice, showing LKS, LT-HSC, ST-HSC and multipotent progenitor (MPP) populations. WT, wild type. **b**, Quantification of HPSC populations assessed by FACS. $*P < 0.05$, error bars represent s.e.m., $n = 3$ per genotype. **c**, Cell cycle analysis of the LT-HSCs in *Aldh2*$^{-/-}$ *Fancd2*$^{-/-}$ mice and controls ($n = 5$ per genotype) determined by Ki-67 and 4′,6-diamidino-2-phenylindole (DAPI) staining. **d**, Frequency of c.f.u.-S_{10} in the bone marrow of *Aldh2*$^{-/-}$ *Fancd2*$^{-/-}$ and control mice. Each point represents the number of c.f.u.-S_{10} counted in the spleen of a single recipient. $n = 20$ per genotype, central line represents the mean, error bars represent the s.e.m., $***P < 0.001$. **e**, Limiting dilution assay was carried out by transplanting six concentrations of mutant bone marrow and a set concentration of wild-type competitor cells (12 recipients were used per test cell dose). Young *Aldh2*$^{-/-}$ *Fancd2*$^{-/-}$ bone marrow exhibited a 638-fold reduction in the frequency of HSCs compared to wild type ($P < 0.0001$).

long-term competitive repopulation assay. This assay allows the frequency of LT-HSCs within mutant bone marrow to be calculated (defined as competitive repopulation units, CRU) and is based on their functional ability to reconstitute all blood lineages in lethally irradiated mice[25]. The data in Fig. 4e and Supplementary Fig. 7c reveal that double-mutant marrow is profoundly compromised, showing a 638-fold reduction in the frequency of CRU compared with wild type ($P < 1 \times 10^{-20}$). It is also worth noting that the long-term repopulating ability in *Aldh2*$^{-/-}$ bone marrow was reduced 2.75-fold ($P = 0.0156$), demonstrating the functional importance of aldehyde dehydrogenase activity associated with the HSC compartment. Furthermore, there was a 38-fold reduction in the HSC pool of *Fancd2*$^{-/-}$ mice compared to wild type ($P = 5 \times 10^{-18}$). It is notable that the combined inactivation of both acetaldehyde catabolism and the Fanconi anaemia DNA-repair pathway leads to a synergistic functional HSC defect.

The data presented here reveal that HSPCs use two parallel mechanisms for protection from the irreversible genetic damage caused by reactive aldehydes. Recently, numerous studies have identified critical roles for a variety of DNA-repair pathways in HSC homeostasis, with defective DNA repair leading to age-dependent dysfunction of these cells in mice[1,2,26,27]. We show that the combined inactivation of aldehyde detoxification and the Fanconi anaemia DNA-repair pathway results in persistent DNA damage in HSCs. This leads to the loss of a functional HSC pool, and precipitates spontaneous bone marrow failure. Children with Fanconi anaemia often succumb to bone marrow failure and leukaemia, in both instances due to genetic damage to the stem cells[9,28]. This study also provides the first evidence, to our knowledge, about what drives the Fanconi anaemia haematological phenotype, and has the potential to inform future therapeutic interventions for this lethal human illness. Perhaps the most important implication of this work is the revelation that naturally produced aldehydes can be potently genotoxic to HSCs, and without the necessary protection, these stem cells malfunction or die, the two key features that typify a process of accelerated ageing.

METHODS SUMMARY

Mice. *Aldh2*$^{-/-}$ *Fancd2*$^{-/-}$ mice were described previously[4]. All animals were maintained in specific pathogen-free conditions. In individual experiments, all mice were matched for age and gender. All animal experiments undertaken in this study were done so with the approval of the UK Home Office.

Haematopoietic progenitor. Survival of lineage-restricted progenitors was assessed using methylcellusose-based media, and survival of short-term HSCs was assessed using the c.f.u.-S assay, as described previously[10–12]. Total bone marrow was treated with acetaldehyde *in vitro* for 4 h before plating in methylcellulose-based media or injection into lethally irradiated recipients (see Methods).

Aldefluor stain. The Aldefluor stain was performed according to the manufacturer's instructions, using bone marrow cells pre-stained for surface markers to define HSCs, as described in Methods. Aldefluor fluorescence was quantified using the geometric mean.

Limiting dilution assay. The limiting dilution assay was performed essentially as described previously[19]. Varying amounts of male 'test' bone marrow (8×10^3, 4×10^4, 2×10^5, 1×10^6, 5×10^6 and 2.5×10^7 cells) were mixed with a fixed amount (2×10^5) of wild-type female bone marrow and injected into lethally irradiated (900 Gy, split between two doses) female F_1 C57B6/Jo1a × 129/SV recipients. Twelve recipients were used for each dose of test bone marrow. After 16 weeks, mice were assessed for multi-lineage reconstitution (see Methods).

Statistical analysis. Unless otherwise stated, data reflect the mean ± s.e.m., and a two-tailed Student's *t*-test was used to assess the statistical significance ($^*P<0.05$, $^{**}P<0.01$, $^{***}P<0.001$, $^{****}P<0.0001$).

Full Methods and any associated references are available in the online version of the paper.

Received 4 April; accepted 29 June 2012.
Published online 26 August 2012.

1. Nijnik, A. *et al.* DNA repair is limiting for haematopoietic stem cells during ageing. *Nature* **447,** 686–690 (2007).
2. Rossi, D. J. *et al.* Deficiencies in DNA damage repair limit the function of haematopoietic stem cells with age. *Nature* **447,** 725–729 (2007).
3. Niedernhofer, L. J. DNA repair is crucial for maintaining hematopoietic stem cell function. *DNA Repair (Amst.)* **7,** 523–529 (2008).
4. Langevin, F., Crossan, G. P., Rosado, I. V., Arends, M. J. & Patel, K. J. Fancd2 counteracts the toxic effects of naturally produced aldehydes in mice. *Nature* **475,** 53–58 (2011).
5. Rosado, I. V., Langevin, F., Crossan, G. P., Takata, M. & Patel, K. J. Formaldehyde catabolism is essential in cells deficient for the Fanconi anemia DNA-repair pathway. *Nature Struct. Mol. Biol.* **18,** 1432–1434 (2011).
6. Rogakou, E. P., Pilch, D. R., Orr, A. H., Ivanova, V. S. & Bonner, W. M. DNA double-stranded breaks induce histone H2AX phosphorylation on serine 139. *J. Biol. Chem.* **273,** 5858–5868 (1998).
7. Houghtaling, S. *et al.* Epithelial cancer in Fanconi anemia complementation group D2 (*Fancd2*) knockout mice. *Genes Dev.* **17,** 2021–2035 (2003).
8. Crossan, G. P. *et al.* Disruption of mouse Slx4, a regulator of structure-specific nucleases, phenocopies Fanconi anemia. *Nature Genet.* **43,** 147–152 (2011).
9. Kutler, D. I. *et al.* A 20-year perspective on the International Fanconi Anemia Registry (IFAR). *Blood* **101,** 1249–1256 (2003).
10. McCulloch, E. A. & Till, J. E. The radiation sensitivity of normal mouse bone marrow cells, determined by quantitative marrow transplantation into irradiated mice. *Radiat. Res.* **13,** 115–125 (1960).
11. Meagher, R. C., Sieber, F. & Spivak, J. L. Suppression of hematopoietic-progenitor-cell proliferation by ethanol and acetaldehyde. *N. Engl. J. Med.* **307,** 845–849 (1982).
12. Becker, A. J., Mc, C. E. & Till, J. E. Cytological demonstration of the clonal nature of spleen colonies derived from transplanted mouse marrow cells. *Nature* **197,** 452–454 (1963).
13. Balber, A. E. Concise review: aldehyde dehydrogenase bright stem and progenitor cell populations from normal tissues: characteristics, activities, and emerging uses in regenerative medicine. *Stem Cells* **29,** 570–575 (2011).
14. Armstrong, L. *et al.* Phenotypic characterization of murine primitive hematopoietic progenitor cells isolated on basis of aldehyde dehydrogenase activity. *Stem Cells* **22,** 1142–1151 (2004).
15. Storms, R. W. *et al.* Distinct hematopoietic progenitor compartments are delineated by the expression of aldehyde dehydrogenase and CD34. *Blood* **106,** 95–102 (2005).
16. Storms, R. W. *et al.* Isolation of primitive human hematopoietic progenitors on the basis of aldehyde dehydrogenase activity. *Proc. Natl Acad. Sci. USA* **96,** 9118–9123 (1999).
17. Levi, B. P., Yilmaz, O. H., Duester, G. & Morrison, S. J. Aldehyde dehydrogenase 1a1 is dispensable for stem cell function in the mouse hematopoietic and nervous systems. *Blood* **113,** 1670–1680 (2009).
18. Hess, D. A. *et al.* Selection based on CD133 and high aldehyde dehydrogenase activity isolates long-term reconstituting human hematopoietic stem cells. *Blood* **107,** 2162–2169 (2006).
19. Kiel, M. J., Yilmaz, O. H., Iwashita, T., Terhorst, C. & Morrison, S. J. SLAM family receptors distinguish hematopoietic stem and progenitor cells and reveal endothelial niches for stem cells. *Cell* **121,** 1109–1121 (2005).
20. Purton, L. E. & Scadden, D. T. Limiting factors in murine hematopoietic stem cell assays. *Cell Stem Cell* **1,** 263–270 (2007).
21. Rossi, D. J. *et al.* Cell intrinsic alterations underlie hematopoietic stem cell aging. *Proc. Natl Acad. Sci. USA* **102,** 9194–9199 (2005).
22. Sudo, K., Ema, H., Morita, Y. & Nakauchi, H. Age-associated characteristics of murine hematopoietic stem cells. *J. Exp. Med.* **192,** 1273–1280 (2000).
23. Wilson, A. *et al.* Hematopoietic stem cells reversibly switch from dormancy to self-renewal during homeostasis and repair. *Cell* **135,** 1118–1129 (2008).
24. Mohrin, M. *et al.* Hematopoietic stem cell quiescence promotes error-prone DNA repair and mutagenesis. *Cell Stem Cell* **7,** 174–185 (2010).
25. Szilvassy, S. J., Humphries, R. K., Lansdorp, P. M., Eaves, A. C. & Eaves, C. J. Quantitative assay for totipotent reconstituting hematopoietic stem cells by a competitive repopulation strategy. *Proc. Natl Acad. Sci. USA* **87,** 8736–8740 (1990).
26. Milyavsky, M. *et al.* A distinctive DNA damage response in human hematopoietic stem cells reveals an apoptosis-independent role for p53 in self-renewal. *Cell Stem Cell* **7,** 186–197 (2010).
27. Seita, J., Rossi, D. J. & Weissman, I. L. Differential DNA damage response in stem and progenitor cells. *Cell Stem Cell* **7,** 145–147 (2010).
28. Crossan, G. P. & Patel, K. J. The Fanconi anaemia pathway orchestrates incisions at sites of crosslinked DNA. *J. Pathol.* **226,** 326–337 (2012).

Supplementary Information is linked to the online version of the paper at www.nature.com/nature.

Acknowledgements We thank M. Grompe for *Fancd2*-deficient mice and M. Milsom and D. Walter for technical advice. We are grateful to T. Langford, R. Berks, A. Middleton, C. Knox and J. Wiles for their help with mouse experimental work. We would also like to thank the Biomed services and ARES staff for animal husbandry and assistance. We thank N. Grant for photography. We thank the Human Research Tissue Bank (NIHR Cambridge Biomedical Research Centre) for processing histology. We also thank F. Zhang for help with FACS. G.P.C. is supported by CRUK and Homerton College, Cambridge. J.I.G. is supported by the Milstein Fund and the Darwin Trust of Edinburgh. F.L. is supported by the March of Dimes Foundation.

Author Contributions The study was conceived by K.J.P., G.P.C. and J.I.G. The manuscript was written by K.J.P., G.P.C. and J.I.G. All experiments were planned and executed by J.I.G. and G.P.C. Cell sorting was performed by M.D. Additional analysis of mice with bone marrow failure was conducted by F.L. M.J.A. analysed histological samples and provided useful discussion.

Author Information Reprints and permissions information is available at www.nature.com/reprints. The authors declare no competing financial interests. Readers are welcome to comment on the online version of this article at www.nature.com/nature. Correspondence and requests for materials should be addressed to K.J.P. (kjp@mrc-lmb.cam.ac.uk).

METHODS

Mice. *Aldh2*$^{-/-}$ *Fancd2*$^{-/-}$ mice on a C57/B6Jo1a × 129SV hybrid background were described previously[4]. *Fancd2*-deficient mice (*Fancd2*^{tm1Hou}, Mouse Genome Informatics (MGI) code: 2673422, 129S4/SvJae) were a gift from M. Grompe. *Aldh2*-deficient mice were generated from embryonic stem (ES) cells obtained from EUCOMM (*Aldh2*$^{tm1a(EUCOMM)Wtsi}$; MGI code: 4431566, C57BL/6N). Mice carrying both the *Fancd2*^{tm1Hou} and *Aldh2*$^{tm1a(EUCOMM)Wtsi}$ synthetic alleles were generated by crossing *Fancd2*^{tm1Hou} and *Aldh2*$^{tm1a(EUCOMM)Wtsi}$ heterozygous mice. These progeny were subsequently intercrossed to obtain double-mutant mice and control genotypes as described previously[4]. *Fanca*-deficient mice were generated from ES cells, carrying a targeted disruption of the *Fanca* locus, obtained from the EUCOMM consortium (Supplementary Fig. 5b). Targeting was confirmed by long-range PCR using the following oligonucleotides. LAR3: CACAACGGGTTCTTCTGTTAGTCC; GF4: GCTAACACTAGTAAGAGTC ACAATAATCTC; RAF5; CACACCTCCCCCTGAACCTGAAAC; and GR3: CTTGTTGGTGGTTGGATATCTTGATGGTTG (Supplementary Fig. 5b). Germline transmission was achieved and progeny were genotyped using the following oligonucletotides. FL033: GCCTTTGCTGCTCTAATTCCATGT; FL040: TCAGCTCACTGAGACGCAACCTTTTACACT; and En2A: GCTTCACTGA GTCTCTGGCATCTC (Supplementary Fig. 5c). Furthermore, cells derived from *Fanca*-deficient mice were unable to mono-ubiquitinate Fancd2 after damage with MMC (Supplementary Fig. 5d). All animals were maintained in specific pathogen-free conditions. In individual experiments all mice were matched for age and gender. All animal experiments undertaken in this study were done so with the approval of the UK Home Office.

Aldefluor stain. Aldefluor stain was performed according to the manufacturer's instructions, using bone marrow cells pre-stained for surface markers to define HSPCs as described below. Fluoresence was quantified using the geometric mean.

Limiting dilution assay. The limiting dilution assay was performed essentially as described previously[19]. Varying amounts of male 'test' bone marrow (8×10^3, 4×10^4, 2×10^5, 1×10^6, 5×10^6 and 2.5×10^7 cells) were mixed with a fixed amount (2×10^5) of wild-type female bone marrow and injected into lethally irradiated (900 Gy, split between two doses) female F_1 C57B6/Jo1a × 129/SV recipients. Twelve recipients were used for each dose of test bone marrow. After 16 weeks, these recipients were killed and peripheral blood was fractionated by FACS into T cells ($CD4^+$ or $CD8^+$, $B220^-$ $Gr\text{-}1^-$ $Mac\text{-}1^-$), B cells ($B220^+$ $CD4^-$ $CD8^-$ $Gr\text{-}1^-$ $Mac\text{-}1^-$) and myeloid cells ($Gr\text{-}1^+$ or $Mac\text{-}1^+$, $B220^-$ $CD4^-$ $CD8^-$) using surface markers described previously[29]. The relative contribution of the test and wild-type bone marrow to peripheral blood chimaerism was then assessed using quantitative PCR (qPCR) for the Y chromosome with oligonucleotides described previously[30]. Recipients were considered reconstituted with test bone marrow if all three lineages showed ≥1% chimaerism for the test bone marrow. The frequency of non-reconstituted mice is plotted against the dose of test cells injected. The frequency of CRU was calculated using L-Calc and *P* values were calculated using ELDA software at http://bioinf.wehi.edu.au/software/elda.

Statistical analysis. Unless otherwise stated, data reflect the mean ± s.e.m., and a two-tailed Student's *t*-test was used to assess the statistical significance ($^*P < 0.05$, $^{**}P < 0.01$, $^{***}P < 0.001$, $^{****}P < 0.0001$).

Histological analysis. Histological analysis was performed on tissues that had been fixed in neutral buffered formalin for 24 h. The samples were then paraffin embedded and 4 μm sections were cut before staining with haematoxylin and eosin. Immohistochemistry was performed as described previously[31], using rabbit anti-phospho-histone H2AX (Cell Signaling 2577; 1:50) and rabbit anti-cleaved caspase-3 (Cell Signaling Asp175 9661L; 1:100).

Peripheral blood. Peripheral blood was collected from mice at 8–12 weeks of age or from aged mice as indicated. Whole blood (50–100 μl) was collected in ETDA microvette tubes (Startedt) and analysed on a VetABC analyser (Horiba).

γ-H2AX staining. γ-H2AX staining by flow cytometry was performed using the total bone marrow of aged mutant mice and appropriate controls. Cells were resuspended at a concentration of 3×10^6 cells per 100 μl. The cells were stained for surface markers using biotin lineage cocktail (Miltenyi Biotec), anti-c-Kit (PerCP-Cy5.5), and anti-Sca-1 (PE-Cy7). The samples were incubated for 15 min at 4 °C in the dark. Anti-Flt3 (PE) and anti-CD34 (eFluor660) were also added to the stain of lineage-depleted bone marrow of young mice, and these samples were incubated for 75 min at 4 °C in the dark. Brilliant violet-421 streptavidin was added and the cells incubated for a further 15 min. Cells were fixed and permeabilized using Intraprep (Beckman Coulter) following the manufacturer's instructions. The cells were then stained for 15 min with a FITC-conjugated anti-γ-H2AX antibody (JBW301, Upstate).

Survival assays of primary mouse B cells. Survival assays of primary mouse B cells were performed with lymphocytes purified from the spleen using Lympholyte M (Cederlane). Lymphocytes were stimulated with LPS (Sigma L4391) at a final concentration of 40 μg ml^{-1}. A total of 4×10^5 cells were plated with acetaldehyde in one well of a 24-well plate. After 7 days the viable cells were enumerated by trypan blue exclusion, counting 100 images using a ViCell XR (Beckman Coulter). Each data point represents the mean of three independent experiments, each carried out in triplicate.

Methylcellulose c.f.u. survival assays. Methylcellulose c.f.u. survival assays were carried out as described previously[10–12]. Briefly, total bone marrow was flushed in IMDM (GIBCO) from the femora and tibiae of mutant mice and controls. The number of nucleated cells was enumerated using a solution of 3% acetic acid and methylene blue, and counted using a ViCell XR Cell counter. Equal numbers of total bone marrow cells were then exposed to various concentrations of acetaldehyde *in vitro* for 4 h in a sealed CryoVial. After treatment, two tenfold serial dilutions of the bone marrow were made, and these cells were plated into 6-well plates with methylcellulose-based media containing cytokines.

For c.f.u.-GM, cells were plated at final concentrations of 2×10^6, 2×10^5 and 2×10^4 cells per well in MethoCult M3534 (StemCell Technologies). Colonies were counted 7 days after incubation at 37 °C and 5% CO_2. For c.f.u.-E, cells were treated in the same manner, but were plated into MethoCult M3334 (StemCell Technologies) and colonies were counted after 2 days. In all cases survival was made relative to the untreated control for each genotype. Each point represents the mean of two independent experiments, each carried out in duplicate.

c.f.u.-S assays. c.f.u.-S assays were performed as described previously[10–12]. To assess the frequency of c.f.u.-S in mutant mice, total bone marrow was flushed from the femora and tibiae of mutant mice and appropriate controls. Nucleated cells were enumerated using a solution of 3% acetic acid and methylene blue. The mutant bone marrow was then injected intravenously into 20 recipient irradiated mice that had been lethally irradiated. 1×10^5 nucleated bone marrow cells were used for wild-type, *Aldh2*$^{-/-}$ and *Fancd2*$^{-/-}$ bone marrow, and 5×10^5 cells for *Aldh2*$^{-/-}$ *Fancd2*$^{-/-}$ bone marrow. After 10 days the spleens were fixed in Bouin's solution (Sigma), the number of colonies were counted and made relative to the number of total bone marrow cells injected.

To assess the survival of c.f.u.-S after exposure to acetaldehyde, we treated total bone marrow cells with various acetaldehyde concentrations for 4 h *in vitro* before injecting them into lethally irradiated recipient mice. After 10 days, the number of c.f.u.-S were counted. The survival was made relative to the untreated control for each genotype. Each data point represents the mean c.f.u.-S survival in eight recipient mice.

Irradiation of mice. Irradiation of mice was performed using a Cs-137 GSR C1m blood irradiator (Gamma-Service Recycling Gmbh; Germany). Mice received a dose of 900 Gy of total body irradiation, split between two equal doses, separated by 4 h. Mice received prophylactic enrofloxacin (Baytril, Bayer) in the drinking water for 7 days before irradiation and for 5 weeks after irradiation.

Flow cytometry. Flow cytometry was performed on bone marrow cells that were isolated from the femora and tibiae of mutant mice and appropriate controls by flushing cells and passing them through a 70-μm filter. The following antibodies were used to stain for HSCs: FITC-conjugated lineage cocktail with antibodies anti-CD4 (clone H129.19, BD Pharmingen), CD3e (clone 145-2C11, eBioscience), Ly-6G/Gr-1 (clone RB6-8C5, eBioscience), CD11b/Mac-1 (clone M1/70, BD Pharmingen), CD45R/B220 (clone RA3-6B2, BD Pharmingen), Fcε R1α (clone MAR-1, eBioscience), CD8a (clone 53-6.7, BD Pharmingen), CD11c (clone N418, eBioscience) and TER-119 (clone Ter119, BD Pharmingen), anti-c-Kit (PerCP-Cy5.5, clone 2B8, eBioscience), anti-Sca-1 (PE-Cy7, clone D7, eBioscience), anti-Flt3 (PE, clone A2F10, eBioscience) and anti-CD34 (eFluor660, clone RAM34, eBioscience). When staining for SLAM markers the same lineage cocktail was used (FITC) with the addition of the following antibodies: anti-CD48 (FITC, clone HM48-1, BioLegend), anti-CD41 (FITC, clone MWReg30, BD Pharmigen), anti-CD150 (APC, clone TC15-12F12.2, BioLegend) and anti-c-Kit and Sca-1 as above. Maturation of B cells was assessed using anti-CD45R/B220 (PE, clone RA3-6B2, BD Pharmingen) and anti-IgM (APC, clone II/41, BD Pharmingen). The maturation of the erythroid lineage was analysed using antibodies anti-TER-119 (APC, clone Ter-119, BD Pharmingen) and anti-CD71 (PE, clone C2, BD Pharmingen). Granulocyte–macrophage maturation was assessed with antibodies anti-CD11b/Mac-1 (APC, clone M1/70, BD Pharmingen) and anti-Ly-6G/Gr-1 (PE, clone RB6-8C5, eBioscience). Thymic T-cell maturation was assessed using CD4 (FITC, clone H129.19, BD Pharmingen) and CD8a (PE, clone 53-6.7, BD Pharmingen) antibodies. For the FACS sorting of peripheral white blood cells the following antibodies were used: anti-CD4 (FITC, clone H129.19, BD Pharmingen), anti-CD8a (FITC, clone 53-6.7, BD Pharmingen), anti-CD45R/B220 (APC, clone RA3-6B2, BD Pharmingen), anti-CD11b/Mac-1 (PE, clone M1/70, BD Pharmingen) and anti-Ly-6G/Gr-1 (PE, clone 1A8, BD Pharmingen). The samples were incubated for 15 min at 4 °C in the dark with the exception of samples containing anti-CD34 (RAM34), which were incubated for 90 min. Samples were run on a

LSRII flow cytometer (BD Pharmingen) and the data were analysed with FlowJo 9.3.1 (Tree Star).

Y chromosome qPCR. Y chromosome qPCR was performed on genomic DNA from total peripheral blood or FACS-sorted peripheral blood cells (T cells ($B220^-$ $Gr\text{-}1^-$ $Mac\text{-}1^-$ $CD4^+$ or $CD8^+$), B cells ($Gr\text{-}1^-$ $Mac\text{-}1^-$ $CD4^-$ $CD8^-$ $B220^+$) or myeloid cells ($CD4^-$ $CD8^-$ $B220^-$ $Gr\text{-}1^+$ or $Mac\text{-}1^+$)) using QIAamp DNA micro kit (Qiagen). qPCR was performed using SYBR GreenER qPCR Supermix (Invitrogen). The level of male chimaerism was calculated using oligonucleotides to amplify the genomic regions of the *Tspy* and β-actin genes and the $\Delta\Delta C_T$ method[30]. qPCR was performed in triplicate using the following conditions: 50 °C for 2 min and 95 °C for 10 min, followed by 50 cycles of 95 °C for 15 s, and 60 °C for 1 min, on a 7900HT Fast Real-Time system (Applied Biosystems).

Ki-67 staining. Ki-67 staining was performed on total bone marrow that was lineage depleted using a magnetic bead lineage depletion kit (Miltenyi Biotec). The cells were then stained for surface markers: biotin lineage cocktail (Miltenyi Biotec), streptavidin (APC-Cy7), c-Kit (PerCP-Cy5.5), Sca-1 (PE-Cy7), CD34 (eFluor660) and Flt3 (PE). The cells were fixed and permeabilized using the Cytofix/Cytoperm kit (BD Pharmigen) following the manufacturer's instructions. The cells were then stained overnight at 4 °C with FITC mouse anti-human Ki-67 (B56, BD Pharmigen). The samples were washed and resuspended in PBS plus 3% FCS with DAPI, at a final concentration of 3 μM, and analysed immediately.

CAFC assay. The CAFC assay was performed on a layer of freshly established wild-type murine stromal cells, as described previously[32]. The stromal layer was cultured at 33 °C and 5% CO_2 until confluency was reached and was then inactivated by irradiation with 15 Gy. Single-cell suspensions of whole bone marrow were prepared at various concentrations and seeded on the stromal layer in 96-well plates with MyeloCult Media (StemCell Technologies) as described previously[32,33]. The plates were incubated at 33 °C and 5% CO_2 for 21 days, and colonies scored as described previously[34]. The CAFC frequency was calculated based on the Poisson distribution using L-Calc software (StemCell Technologies).

29. Ema, H. *et al.* Adult mouse hematopoietic stem cells: purification and single-cell assays. *Nature Protocols* **1,** 2979–2987 (2006).
30. Wang, L. J. *et al.* Engraftment assessment in human and mouse liver tissue after sex-mismatched liver cell transplantation by real-time quantitative PCR for Y chromosome sequences. *Liver Transpl.* **8,** 822–828 (2002).
31. Drost, R. *et al.* BRCA1 RING function is essential for tumor suppression but dispensable for therapy resistance. *Cancer Cell* **20,** 797–809 (2011).
32. Lo Celso, C., Klein, R. J. & Scadden, D. T. Analysis of the hematopoietic stem cell niche. *Curr. Protoc. Stem Cell Biol.* Chapter 2, Unit 2A 5 (2007).
33. Zhang, Q. S. *et al. Fancd2*$^{-/-}$ mice have hematopoietic defects that can be partially corrected by resveratrol. *Blood* **116,** 5140–5148 (2010).
34. Amrani, Y. M. *et al.* The *Paf* oncogene is essential for hematopoietic stem cell function and development. *J. Exp. Med.* **208,** 1757–1765 (2011).